Human Molecular Genetics, 2004, Vol. 13, No. 24 ***3171–3179***
doi:10.1093/hmg/ddh326
Advance Access published on October 20, 2004

Heterologous mitochondrial DNA recombination in human cells

Marilena D'Aurelio[1], Carl D. Gajewski[1], Michael T. Lin[1], William M. Mauck[1], Leon Z. Shao[1], Giorgio Lenaz[2], Carlos T. Moraes[3] and Giovanni Manfredi[1,*]

[1]Department of Neurology and Neuroscience, Weill Medical College of Cornell University, New York, NY, USA, [2]Dipartimento di Biochimica, G. Moruzzi, Università di Bologna, Italy and [3]Department of Neurology, University of Miami School of Medicine, Miami, FL, USA

Received August 25, 2004; Revised and Accepted October 11, 2004

Inter-molecular heterologous mitochondrial DNA (mtDNA) recombination is known to occur in yeast and plants. Nevertheless, its occurrence in human cells is still controversial. To address this issue we have fused two human cytoplasmic hybrid cell lines, each containing a distinct pathogenic mtDNA mutation and specific sets of genetic markers. In this hybrid model, we found direct evidence of recombination between these two mtDNA haplotypes. Recombinant mtDNA molecules in the hybrid cells were identified using three independent experimental approaches. First, recombinant molecules containing genetic markers from both parental alleles were demonstrated with restriction fragment length polymorphism of polymerase chain reaction products, by measuring the relative frequencies of each marker. Second, fragments of recombinant mtDNA were cloned and sequenced to identify the regions involved in the recombination events. Finally, recombinant molecules were demonstrated directly by Southern blot using appropriate combinations of polymorphic restriction sites and probes. This combined approach confirmed the existence of heterogeneous species of recombinant mtDNA molecules in the hybrid cells. These findings have important implications for mtDNA-related diseases, the interpretation of human evolution and population genetics and forensic analyses based on mtDNA genotyping.

INTRODUCTION

Mitochondrial DNA (mtDNA) recombination has been well documented in plants, fungi and protists (1) and in invertebrates (2), and the activity of enzymes involved in homologous recombination has been identified in mammalian mitochondria (3). However, despite ample evidence of intramolecular mtDNA recombination (4,5), the existence of inter-molecular mtDNA recombination in mammalian cells is still controversial, since most studies are based on indirect evidence derived from statistical analyses of mtDNA sequence data (6–8).

Recently, inter-molecular heterologous recombination between paternal and maternal mtDNA molecules has been reported in a patient suffering from a form of mitochondrial myopathy, who had a unique case of biparental inheritance of skeletal muscle mtDNA (9). However, except for these very rare cases, recombination events occurring in the normal homoplasmic environment established by maternal uniparental inheritance would go undetected. Therefore, to study mtDNA recombination in human cells we have generated a hybrid cell culture model by fusing two cell lines with similar nuclear background, each harboring a distinct homoplasmic pathogenic mutation in an mtDNA polypeptide-coding gene. Since each mutation individually abolished mitochondrial oxidative phosphorylation, this model allowed us to select for hybrids where mitochondrial function was rescued by the functional interaction among the mutant genomes. At the same time, the mutations provided us with appropriate genetic markers to detect mtDNA recombination between the two species of mutant mtDNA.

RESULTS

Hybrid cells

A scheme of the strategy used for generating the hybrids is shown in Figure 1. We have utilized two lines of

*To whom correspondence should be addressed at: Weill Medical College of Cornell University, 525 E 68th Street, A-505, New York, NY 10021, USA. Tel: +1 2127464605; Fax: +1 2127464803; Email: gim2004@mail.med.cornell.edu

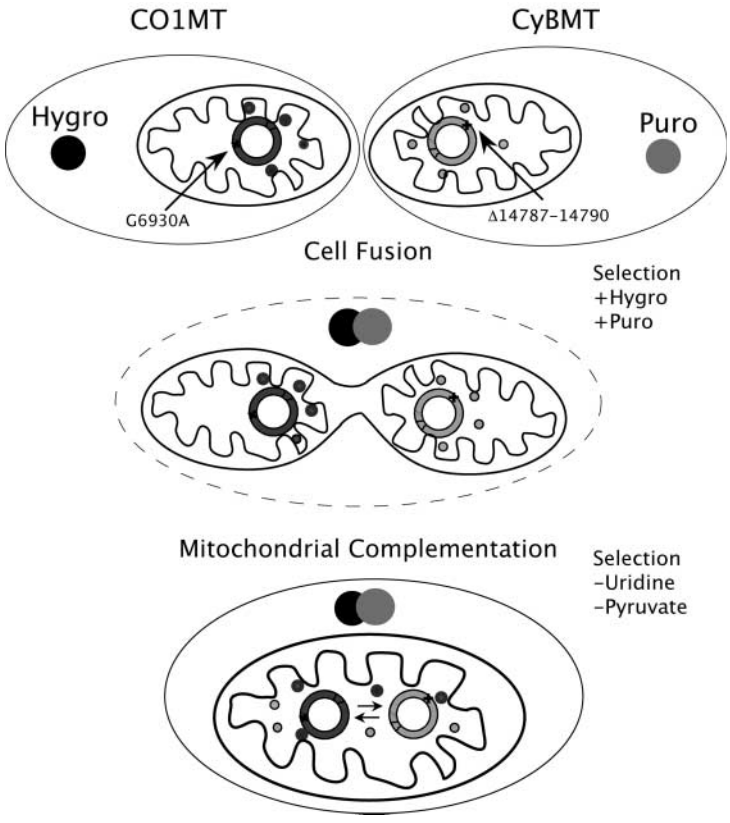

Figure 1. Strategy for the generation of *CO1*MT–*Cy*BMT hybrids. *CO1*MT cybrids homoplasmic for the G6930A mtDNA mutation (dark gray circles) were resistant to the antibiotic hygromycin (Hygro). *CyB*MT cybrids homoplasmic for the 14787–14790 deletion (light gray circles) were resistant to the antibiotic puromycin (Puro). *CO1*MT and *CyB*MT cybrids were fused, and hybrids were selected in hygromycin plus puromycin. *CO1*MT and *CyB*MT cybrids were unable to grow in medium lacking uridine and pyruvate because they lack a functional mitochondrial respiratory chain (10). Therefore, we selected for hybrid clones with mitochondrial functional complementation by growing them in medium lacking uridine and pyruvate. Mitochondrial functional complementation is symbolized by the diffusion of mtDNA-encoded proteins (light and dark gray small circles) within fused mitochondria containing different mtDNA haplotypes.

cytoplasmic hybrids (cybrids) derived from human ρ^0 143B/206 osteosarcoma cells lacking mtDNA (10). One line was repopulated with mtDNA from a patient harboring a G6930A transition (11) creating a stop codon in the gene encoding cytochrome *c* oxidase subunit I (*MTCO1*; accession no. NM_173704). Cybrids containing homoplasmic *MTCO1* mutant (*CO1*MT) mtDNA were completely devoid of MTCO1 protein, lacked cytochrome *c* oxidase (COX) activity and were unable to perform oxidative phosphorylation (12).

The second cybrid line was repopulated with mtDNA from a patient harboring a 4 bp deletion of mtDNA nucleotides 14787–14790, which causes a frame-shift in the gene encoding cytochrome *B* (*MTCyB*; accession no. AF254896), resulting in a truncated protein (13). Cybrids homoplasmic for the *MTCyB* mutation (*CyB*MT) were completely defective in complex III (ubiquinol–cytochrome *c* oxidoreductase) activity and lacked oxidative phosphorylation (14). *CO1*MT cybrids were stably transfected with a plasmid conferring resistance to the antibiotic hygromycin. *CyB*MT cybrids were stably transfected with a plasmid conferring resistance to the antibiotic puromycin. *CO1*MT and *CyB*MT cybrids were fused and the resulting hybrids were selected in puromycin plus hygromycin.

Both *CO1*MT and *CyB*MT cybrids were unable to grow in medium without uridine and pyruvate because they lacked a functional mitochondrial respiratory chain (10). Therefore, after a recovery period in normal medium, we grew hybrid cells in selective medium lacking uridine and pyruvate to select for hybrid clones with restored mitochondrial respiratory chain. Resistant hybrid clones were obtained with selection starting 10 days after fusion, and there was no increase in the frequency of viable clones when the selection was started after 13, 17 and 20 days.

The hybrid clones showed improved mitochondrial respiration (i.e. oxygen consumption) when compared with the parental *CO1*MT and *CyB*MT cybrids. In most hybrid lines, mitochondrial respiration was restored to levels comparable to that of 143B osteosarcoma cells, the progenitors of the ρ^0 143B/206 cells harboring wild-type mtDNA (data not shown). This suggested that the coexistence of the two mutant mtDNA species allowed for mitochondrial functional complementation.

MtDNA haplotypes

We determined the relative proportions of each mtDNA species (i.e. *CO1*MT and *CyB*MT mtDNAs) in the hybrid

clones by restriction fragment length polymorphism (RFLP) analyses of polymerase chain reaction (PCR)-amplified mtDNA. The G6930A transition in the *MTCO1* gene, in combination with a mismatch primer, creates a novel *Alu*I site (11). The 4 bp deletion at nucleotides 14787–14790 in the *MTCyB* gene eliminates a naturally occurring *Ase*I site (14) (Fig. 2A).

Every clone analyzed harbored a mixture of the two mutant mtDNAs. Theoretically, if each hybrid clone harbored a heteroplasmic mixture of only two species of mtDNA, *CO1*MT and *CyB*MT, the sum of these two species should account for 100% of the mtDNA genomes contained in a clone. Furthermore, since the *Alu*I and the *Ase*I sites are linked loci in the *CO1*MT haplotype, the relative proportions of these two genetic markers should always be equal. Likewise, the relative proportion of *Alu*I-negative and *Ase*I-negative mtDNA derived from *CyB*MT should coincide. Instead, we found that in the hybrid clones there was a discrepancy in the proportions of mtDNA digested by *Alu*I and *Ase*I (Fig. 2B and C). In a total of 23 clones analyzed, the average discrepancy was 10% (standard deviation, $\pm 8\%$).

In order to identify additional genetic markers that could distinguish between *CO1*MT and *CyB*MT mtDNA, we sequenced a portion of the D-loop region from both parental cybrids. Among several nucleotide variations in this region, we identified a C16278T transition in the *CO1*MT mtDNA creating a novel *Eco*RV site. Using primers P5 and P6 (Fig. 3A) we amplified a 267 bp mtDNA fragment. *Eco*RV digests *CO1*MT mtDNA into two fragments of 130 and 137 bp, respectively. Thus, we measured by PCR–RFLP the relative proportions of *Eco*RV-positive mtDNA in the hybrid clones. Also in this case there was a clear discrepancy between the proportion of *Alu*I-positive and *Eco*RV-positive mtDNA in all the hybrid clones (Fig. 2D).

The *Ase*I and the *Eco*RV markers were much closer to each other (1492 bp apart) than the *Ase*I and the *Alu*I markers (8713 bp apart). Consistent with a model involving recombination between *CO1*MT and *CyB*MT mtDNAs, the discrepancy between the *Alu*I-positive and *Ase*I-positive proportions was greater than the discrepancy between *Eco*RV-positive and *Ase*I-positive proportions.

To exclude that the relative proportions of each mutated mtDNA species in the hybrid clones were miscalculated because of PCR–RFLP artifacts resulting from the coexistence of two genomes, we mixed total genomic DNA from the two parental cybrids in varying proportions. As expected, in this mixing experiment the relative proportions of *Alu*I-positive and *Ase*I-positive mtDNA coincided. When we plotted the data obtained from the mixing experiment, we obtained a regression curve indicating a linear correlation ($y = 1.09x$, $R^2 = 0.98$; Fig. 2E). The slope of 1.09 did not differ significantly from the predicted theoretical slope of 1, when $x = y$ ($P = 0.40$). In contrast, the plot obtained from the hybrid clones showed that x differed from y ($y = 1.7x$, $R^2 = 0.98$; Fig. 2E). The slope of 1.7 deviated significantly from the slope predicted by $x = y$ ($P < 5 \times 10^{-8}$). This supported the concept that in the hybrid clones there were novel recombinant mtDNA molecules in addition to *CO1*MT and *CyB*MT.

Recombinant mtDNA molecules

In order to characterize recombinant mtDNA species at the single molecule level, we generated long-PCR products from two hybrid clones (clones 13-11 and 20-1), encompassing both the *Alu*I site (associated with *CO1*MT) and the *Ase*I site (associated with *CyB*MT) to be subcloned and sequenced. We first amplified long mtDNA fragments from nucleotide 6744 to 14840 and from nucleotide 14747 to 6960. However, we failed to subclone these fragments in *Escherichia coli*, presumably because they contained a 'poison sequence' in and around the *MTCyB* gene that cannot be subcloned with standard techniques (15,16). Finally, we succeeded in amplifying and subcloning a 7386 mtDNA fragment from nucleotide 16144 to 6960, encompassing the *Alu*I site and the *Eco*RV site (associated with *CO1*MT; Fig. 3A). Among 12 subclones, which were analyzed by RFLP and by direct sequencing, we identified two recombinant subclones that did not contain the *Alu*I site but contained the *Eco*RV site, and one recombinant subclone containing the *Alu*I site but not the *Eco*RV site (Fig. 3B). To exclude that these recombinant subclones were the result of a long-PCR artifact, we repeated the same amplification and cloning procedures using as starting templates genomic DNA from *CO1*MT and *CyB*MT parental cybrids mixed in equal proportions. We analyzed 54 subclones from this negative control amplification and none showed discrepancies between the mtDNA markers.

We sequenced the three recombinant mtDNA subclones and compared them to the two parental mtDNA. Including the *Alu*I and the *Eco*RV sites there were 20 polymorphic markers that distinguished the two parental mtDNAs. On the basis of these polymorphisms, we determined that the three recombinant mtDNA molecules were the result of independent recombination events, because the region where the sequence transitioned from *CO1*MT to *CyB*MT differed in each of them (Fig. 3C).

To obtain hybrid clones enriched for recombinant mtDNA, we subjected hybrid clones 13-11 and 20-1, which had a high level of discrepancy between the proportion of *Alu*I-positive and *Ase*I-positive mtDNA, to prolonged treatment with ethidium bromide. By decreasing the mtDNA copy number, ethidium bromide increases the likelihood of skewed mitotic segregation of the mtDNAs in dividing cells (17). After 3 weeks of ethidium bromide treatment (50 ng/ml), cells were subcloned and mtDNA was allowed to repopulate the cells.

Southern hybridization was used to test whether recombinant molecules were detectable with another method. We analyzed 13 ethidium bromide-treated hybrid subclones and the parental cybrids. MtDNA was digested with both *Eco*RV and *Ase*I and probed with an mtDNA fragment spanning nucleotides 15494–16255 and encompassing a region between the polymorphic *Eco*RV and *Ase*I sites. Figure 4 shows a Southern hybridization experiment where recombinant mtDNA was detected. As anticipated, we identified two major bands: one of 3910 bp corresponding to *CyB*MT mtDNA and another of 1492 bp corresponding to *CO1*MT mtDNA (Fig. 4A and B, top). All the hybrid subclones contained both bands, indicating that they were heteroplasmic. In two subclones (13-11-eb2 and 13-11-eb1), there were prominent bands that were not seen in the parental cybrids,

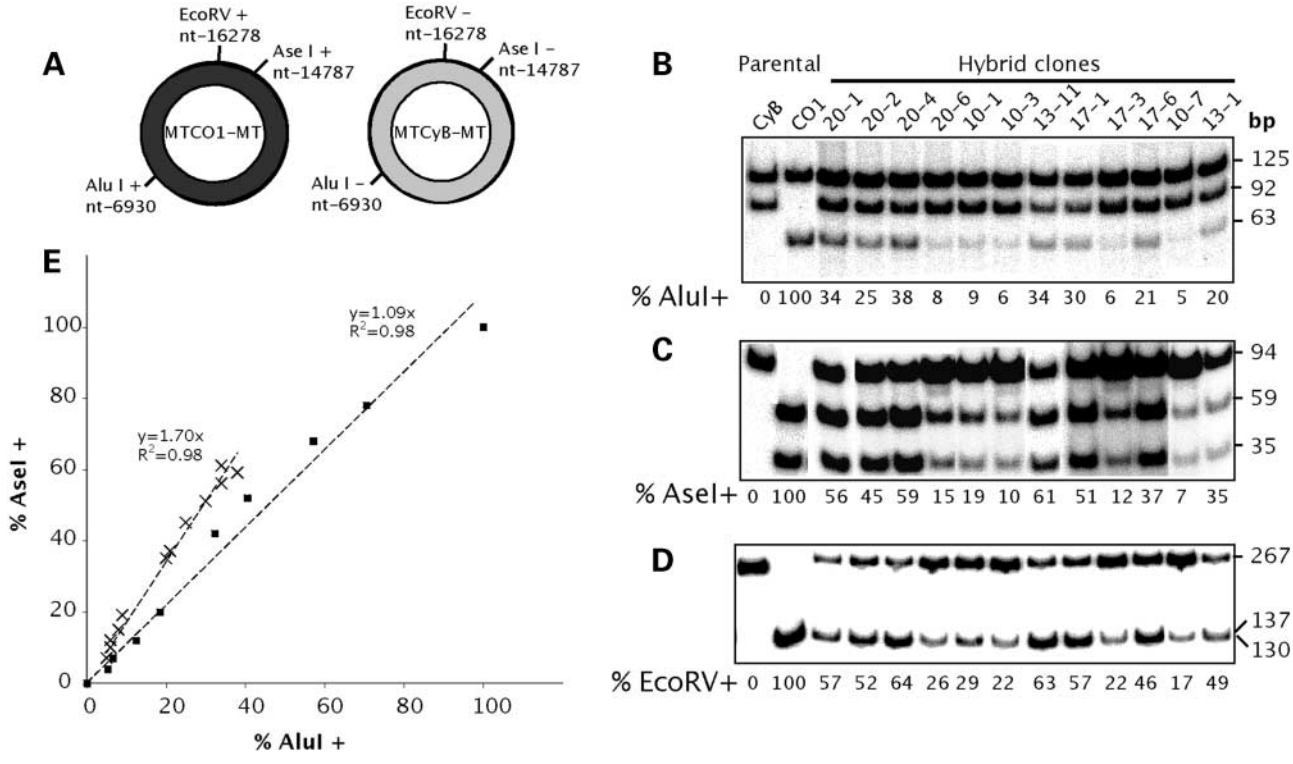

Figure 2. PCR–RFLP quantification of mtDNA alleles in hybrid clones. (**A**) The G6930A transition in *CO1*MT mtDNA (dark gray circle) generates a novel *Alu*I site in conjunction with a mismatch forward PCR primer (11). In addition, *CO1*MT mtDNA contains a polymorphic *Eco*RV site at position 16278. The 14787–14790 deletion in *CyB*MT mtDNA (light gray circle) abolishes a natural *Ase*I site at position 14787 (13). These polymorphic restriction sites were used to calculate the relative proportions of *CO1*MT and *CyB*MT mtDNA in the hybrid clones. (**B**) PCR–RFLP quantification of the proportion of *Alu*I-positive mtDNA. (**C**) PCR–RFLP quantification of the proportion of *Ase*I-positive mtDNA. (**D**) PCR–RFLP quantification of the proportion of *Eco*RV-positive mtDNA. CyB indicates homoplasmic *CyB*MT parental DNA. CO1 indicates homoplasmic *CO1*MT parental DNA. Hybrid clones are labeled according to the number of days after fusion before the beginning of selection in medium lacking uridine and pyruvate followed by the clone number. The percentages of digested PCR products are indicated at the bottom of each lane. In (B), (C) and (D), 12 clones are shown out of a total of 23 clones analyzed. (**E**) The relative proportions of *Alu*I-positive and A*se*I-positive mtDNAs from the hybrid clones are plotted against each other (crosses) and compared with a DNA mixing experiment where *CO1*MT and *CyB*MT parental DNAs were mixed in various proportions (squares). The best fit linear equations and the R^2 values are shown for each curve.

corresponding to the 3407 bp and the 1995 bp fragments derived from mtDNA recombination occurring between the polymoprphic *Eco*RV and *Ase*I sites. To confirm the identity of these bands, the blot was stripped and reprobed with an mtDNA fragment spanning nucleotides 13714–14749 that did not encompass the region between the polymorphic *Eco*RV and *Ase*I sites (Fig. 4A). As expected, with this probe the 1995 bp recombinant band disappeared whereas the 3407 bp one remained (Fig. 4B, bottom). By phosphorimager determination, the relative amounts of the two recombinant bands were ~10% of the total mtDNA. These proportions were very close to the proportions of recombinant mtDNA estimated by PCR–RFLP in the same subclones. Two other subclones (20-1-eb11 and 20-1-eb5) contained lower amounts of the recombinant bands (≤1% of the total mtDNA). Table 1 summarizes the proportions of recombinant mtDNA measured by Southern hybridization and PCR–RFLP in the four ethidium bromide-treated hybrid subclones containing detectable amounts of recombinant mtDNA.

After ethidium bromide treatment, we studied the distribution of mtDNA alleles in hybrid subclones repopulated in medium with and without uridine. The treatment of clone 13-11 resulted in the enrichment for recombinant molecules in several of the subclones containing heteroplasmic mtDNA, as suggested by the distance from a theoretical *Alu*I/*Ase*I linear plot (Fig. 5A). Clone 20-1 yielded similar results (data not shown).

The selection in medium without uridine eliminated all the subclones that contained homoplasmic mutant mtDNA and those that had become ρ^0. Furthermore, we found no clones with proportions of *Alu*I-positive (*CO1*MT) mtDNA higher than 20% in this medium, suggesting that the G6930A *CO*I mutation is more detrimental for oxidative phosphorylation than the *Cy*B mutation. In the presence of uridine, ~50% of the clones had become ρ^0, and several homoplasmic *CO1*MT or *CyB*MT clones were identified.

In all heteroplasmic subclones, the proportion of *Ase*I positivity exceeded the proportion of *Alu*I positivity (Fig. 5A), indicating that the population of double wild-type recombinant molecules (*Ase*I-positive, *Alu*I-negative) exceeded that of the double mutant molecules (*Alu*I-positive, *Ase*I-negative) (Fig. 5B).

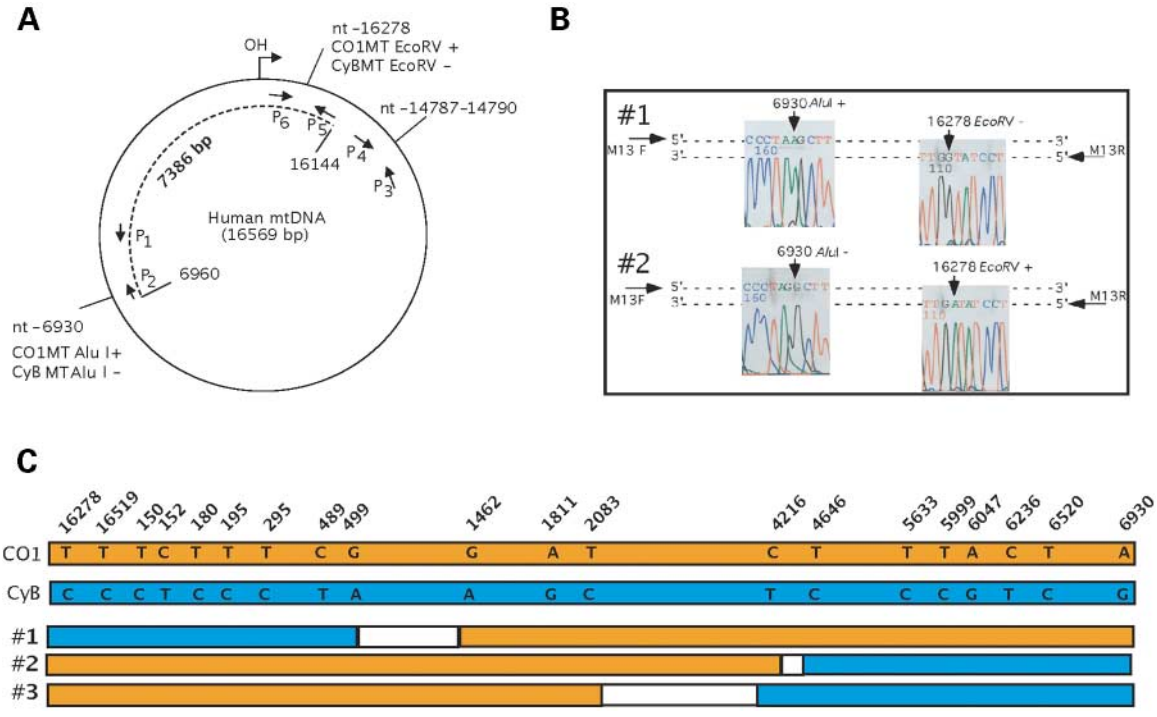

Figure 3. Cloning and sequencing of recombinant mtDNA molecules. (**A**) Diagram of the human mtDNA indicating the positions of the restriction sites and the PCR primers utilized in this work. OH, origin of heavy strand replication. The dashed line represents the 7386 bp-long PCR fragment generated with primers P2–P5 from hybrid clones 20-1 and 13-11 and from *CO1*MT and *CyB*MT parental cybrids. PCR fragments were cloned in *E. coli* and sequenced in their entirety. (**B**) Sequence electropherograms of the mtDNA regions encompassing the *Alu*I and *Eco*RV sites. Recombinant molecule 1 harbors an *Alu*I-positive site from *CO1*MT and an *Eco*RV-negative site from *CyB*MT. Recombinant molecule 2 harbors an *Alu*I-negative site from *CyB*MT and an *Eco*RV-positive site from *CO1*MT. (**C**) Map of mtDNA polymorphisms of the cloned 7386 bp-long regions from *CO1*MT (orange) and *CyB*MT (blue) parental cybrids and three recombinant molecules (orange–blue). In white are the regions of the recombinant molecules whose parental origin could not be determined due to lack of polymorphic sites.

DISCUSSION

There is evidence that supports the concept that human mitochondria possess some of the enzymatic components necessary for homologous recombination (3,18) and that mtDNA can undergo intra-molecular recombination (4,5). However, the identification of inter-molecular mtDNA recombination has been extremely difficult. Recombination within heteroplasmic cells may not result in a detectable haplotype variant unless two distinct non-allelic mutations, coexisting in the same mitochondrion but in different mtDNAs, give rise to novel molecules. In addition, human mtDNA inter-molecular recombination may be an extremely rare event.

Our hybrid human cell system provides an ideal setting to investigate the existence of inter-molecular mtDNA recombination, because it involves mtDNA markers that can easily be recognized by RFLP analyses. We found that the majority of hybrid clones harbored recombinant molecules, which represented a significant proportion of the total mtDNA pool, and that the amount of recombination was highest in those clones where the two parental molecules had segregated in similar proportions. This observation fits a bimolecular reaction model where the probability that two distinct alleles recombine is proportional to the product of the frequency of each allele (i.e. probability of recombination $\propto$ %*CO1*MT $\times$ % *CyB*MT).

On the basis of the PCR–RFLP quantification, in the hybrid clones there was a prevalence of *Alu*I-negative (i.e. *CO1* wild-type) and *Ase*I-positive (i.e. *CyB* wild-type) alleles (Figs 2E and 5). It is possible that, when mtDNA recombination took place the growth conditions resulted in a growth advantage for cells containing these recombinant double wild-type alleles over those containing a high proportion of mutant alleles. However, there was no apparent correlation between the beginning of metabolic selection and the proportion of double wild-type recombinant molecules. For example, in hybrid clone 20-1, which had one of the highest proportions of double wild-type recombinant molecules (Fig. 2B and C), the metabolic selection did not start until day 20 after fusion. After this long time of recovery, the hybrid clones had already established a full complement of mtDNA molecules. Alternatively, the prevalence of double wild-type recombinant mtDNA molecules could result from a replicative advantage of these mtDNAs over the double mutant molecules.

The prolonged ethidium bromide treatment of heteroplasmic hybrid clones in the absence of selection resulted in numerous clones that had either lost their mtDNA or were homoplasmic for one of the two parental mutant mtDNAs.

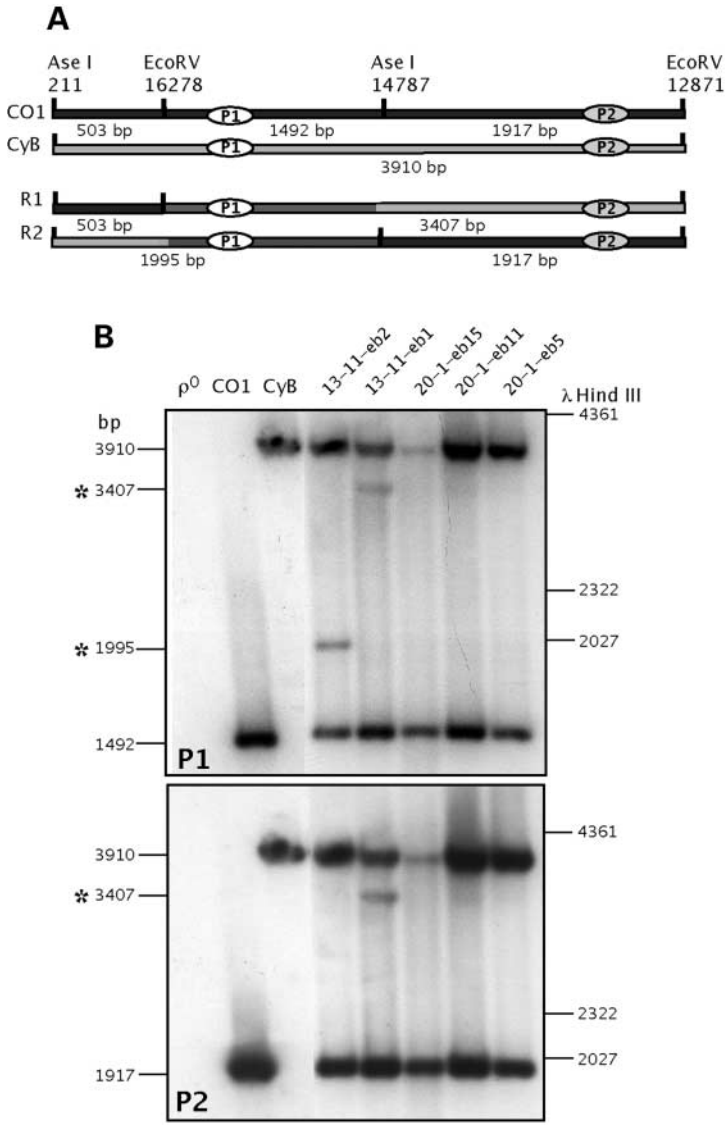

Figure 4. Southern blot of recombinant mtDNA molecules. (**A**) Diagrams of the *Eco*RV and *Ase*I restriction sites (and resulting mtDNA fragments) in the D-loop region of *CO1*MT (CO1, dark gray) and *CyB*MT (CyB, light gray) parental cybrids. The expected restriction fragments generated by recombinant events occurring between the polymorphic *Eco*RV 16278 and *Ase*I 14787 sites are indicated (R1 and R2). The region between the polymorphic markers where recombination has taken place is depicted by an intermediate shade of gray. The nucleotide positions of mtDNA probes P1 and P2 were 15494–16225 and 13714–14749, respectively. (**B**) Radiograms of Southern blots of mtDNA double digested with *Eco*RV and *Ase*I and probed with P1 (top). To ensure specificity of the bands the same membrane was stripped and reprobed with P2 (bottom). Lane ρ^0, DNA from cells lacking mtDNA. Lane CO1, DNA from the parental *CO1*MT cybrids. Lane CyB, DNA from the parental *CyB*MT cybrids. The remaining lanes contain DNA from subclones of ethidium bromide-treated hybrid clones 13-11 and 20-1. In this Southern hybridization experiment five subclones are shown out of a total of 13 analyzed. The molecular weights of the bands of interest are shown at left. λ*Hin*dIII DNA positions are shown at right. The asterisks indicate the bands resulting from digestion of recombinant mtDNA molecules.

This indicates that the treatment effectively lowered mtDNA copy number resulting in skewed mtDNA segregation. However, we did not isolate any clones that contained purely recombinant mtDNA, such as homoplasmic *Alu*I-positive *Ase*I-negative or vice versa. It appears to be very difficult to separate recombinant molecules from the parental molecules. This observation supports the following model to explain the dynamics of mtDNA recombination in the hybrids (Fig. 6). As previously shown, upon cell fusion, cybrids undergo a rapid and dynamic reshaping of the mitochondrial network, characterized by membrane fusion with exchange of diffusible proteins (19). Cybrid mtDNA is thought to be organized in discrete clusters of fewer than eight molecules which are physically assembled and function as 'replicative units', also known as nucleoids (20,21). Earlier studies suggested that nucleoids deriving from different human cybrids do not mix (20). Recently, it was shown that in human cultured cells nucleoids move in a constrained random walk within the mitochondria and, during this motion, they constantly fuse and split (22). The occurrence

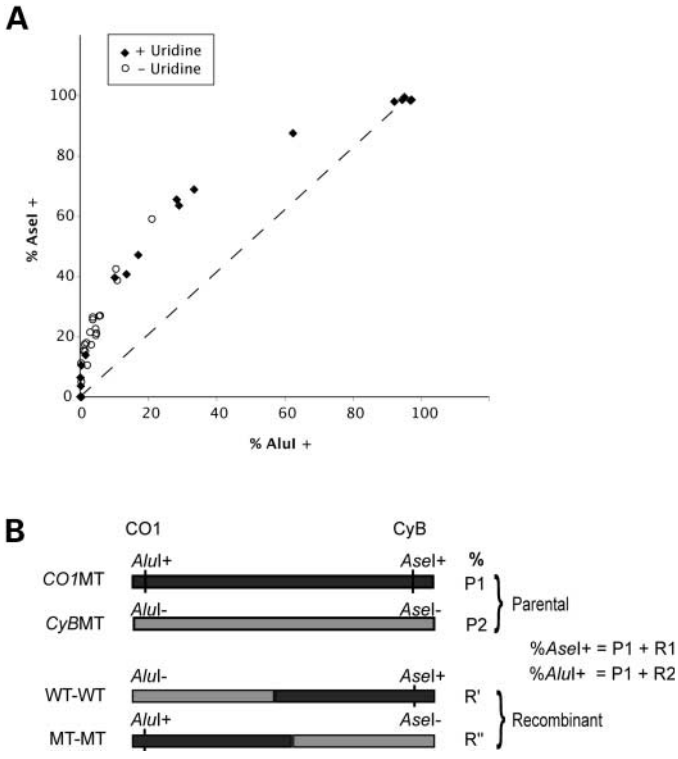

Figure 5. Distribution of mtDNA alleles in hybrid subclones. Subclones of hybrid clone 13-11 were obtained after mtDNA depletion with ethidium bromide for 20 days followed by mtDNA repopulation in the presence (filled diamonds) or in the absence of uridine (empty circles). (**A**) The relative proportions of *Alu*I-positive and *Ase*I-positive mtDNA were measured by PCR–RFLP (as in Fig. 2) and plotted against each other. The dashed line represents the expected distribution of mtDNA alleles in the hybrid subclones in the absence of mtDNA heterologous recombination (such as in the mixing experiment of Fig. 2E). (**B**) In the hypothetical absence of heterologous recombination $R' = R'' = 0$, so the % *Alu*I-positive = P1 = % *Ase*I-positive. However, in all heteroplasmic subclones, we observed that % *Ase*I-positive ≥ %*Alu*I-positive, indicating that $R' \neq 0$ and that $R' \geq R''$.

Table 1. Percentages of mtDNA molecules with recombination between the *EcoRV* (16278) and the *AseI* (14787) restriction sites (four out of 13 total subclones examined by PCR–RFLP and by Southern hybridization)

EB treated subclone	PCR–RFLP (*Eco* RV *Ase* I discrepancy)	Southern hybridization
13-11-eb1	7	11
13-11-eb2	6	9
20-1-eb11	2	1
20-1-eb5	1	<1

of mtDNA recombination in our hybrids indicates that nucleoids from the parental cybrids must have come in very close physical contact to exchange genetic material. Therefore, we propose that after mitochondrial fusion nucleoids are subject to remodeling. During mtDNA replication, only recombination occurring in mixed nucleoids will result in novel mtDNA molecules. It follows that rearranged nucleoids would generate novel species of nucleoids containing a

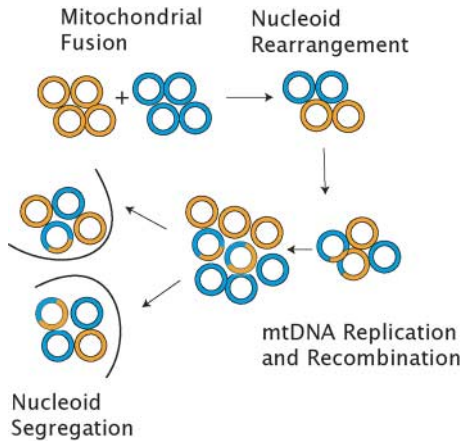

Figure 6. Model of mtDNA distribution in *CO1*MT–*CyB*MT hybrid cells. In this model, mtDNA in hybrid human cells is organized in replicating units or 'nucleoids'. Upon mitochondrial fusion, homoplasmic nucleoids containing different polymorphic markers (blue and orange circles) get in contact with each other and rearrange their composition by exchanging mtDNA molecules. During mtDNA replication or repair within heteroplasmic nucleoids, recombination takes place among different mtDNA haplotypes. Nucleoids containing recombinant molecules can be maintained within the same hybrid cell with no apparent change in mtDNA distribution in the hybrid cells, or they can be randomly distributed in daughter cells, resulting in the segregation of recombinant mtDNA molecules in different hybrid clones.

mixture of parental and recombinant mtDNA. Upon cell division, such novel nucleoids become segregated in daughter cells. The ethidium bromide treatment of hybrid clones presumably resulted in mtDNA depletion to the level of a single nucleoid per cell. Since each nucleoid containing recombinant mtDNA must also contain parental mtDNA, upon mtDNA repopulation, cells will harbor a heteroplasmic mix of parental and recombinant mtDNA.

We have shown that when it is investigated using a system with appropriate genetic markers, products of a variety of mtDNA inter-molecular recombination events can be detected in human tumor cells. Within individual hybrid clones there were different recombinant molecules, suggesting that recombination events involve different mtDNA regions. Previous results in human muscle suggested that the D-loop is a 'hot spot' for mtDNA inter-molecular recombination (9). Our results confirmed that relatively high levels of recombinant mtDNA, detectable by Southern blot, derived from D-loop recombination events. The existence and the mechanisms leading to mtDNA recombination 'hot spots' remain to be determined.

The ability to recombine genetic material among mtDNAs harboring different mutations may be a potential line of defense against the accumulation of pathogenic somatic or inherited mtDNA mutations. Furthermore, the demonstration that mtDNA recombination is an extensive and frequent phenomenon has important implications for studies that employ mtDNA haplotypes as a forensic tool or as an evolutionary 'clock'. MtDNA recombination would have evolutionary significance not only in the rare cases when paternal transmission of mtDNA occurs, but also when an oocyte contains multiple heteroplasmic mtDNA mutations arising spontaneously without paternal contributions. The ability to generate

novel mtDNA molecules by recombination in this situation will necessarily influence the kinds of different mtDNA molecules that will segregate into future generations.

MATERIALS AND METHODS

Hybrid cells

Two lines of cytoplasmic hybrids (cybrids) derived from human ρ^0 143B/206 osteosarcoma cells lacking mtDNA (10) were used. One line was repopulated with mtDNA from a patient harboring a G6930A transition (11) creating a stop codon in *MTCO1*. The second cybrid line was repopulated with mtDNA from a patient harboring a 4 bp deletion of mtDNA nucleotides 14787–14790, which causes a frameshift in *MTCyB*, resulting in a truncated protein (13).

Parental *CO1*MT and *CyB*MT cybrid lines were cultured in Dulbecco's modified Eagle's medium (DMEM) supplemented with 10% fetal bovine serum (FBS) and 50 μg/ml uridine. *CO1*MT cybrids were transfected with the hygromycin resistance conferring plasmid pCDNA3.1-Hygro (Invitrogen) and selected in medium containing 200 μg/ml hygromycin B (Invitrogen). *CyB*MT cybrids were transfected with the puromycin resistance conferring plasmid pIRESpuro (Clontech BD) and selected with 1 μg/ml puromycin (Invitrogen). Cell fusions were carried out in the presence of 50% (w/v) polyethylene glycol 1500 (PEG, American Type Culture Catalog) as described earlier (10). The resulting hybrids were cultured for 3 days without drug selection. Starting on the third day post-fusion, hybrid cells were selected with both puromycin and hygromycin B. After 10, 13, 17 and 20 days post-fusion, nutritional selection of the hybrids was initiated in medium without pyruvate and uridine supplemented with 10% dialysed FBS. Colonies grown in the nutritional selection medium were cloned by the cylinder method and expanded in the same medium as mentioned earlier. Two hybrid clones (20-1 and 13-11) were treated with 50 ng/ml ethidium bromide (17) for 20 days followed by culture in medium with or without uridine supplementation.

Oxygen consumption in the hybrids was measured on intact cells with and without 2 μM of the protonophore carbonyl cyanide *p*-trifluoromethoxyphenylhydrazone (FCCP) in an oxygraph chamber equipped with a Clark-type electrode as described earlier (12).

MtDNA analyses

The sequences of mtDNA primers in Figure 3 were (5′–3′): P1 (nucleotides 6744–6771) ggcttcctagggtttatcgtgtgagcac; P2 (nucleotides 6989–6960) ggccacctacggtgaaaagaaagatgaagc; P3 (nucleotides 14747–14771) atgaccccaatacgcaaaattaac; P4 (nucleotides 14840–14816) ttcatcatgcggagatgttggatg; P5 (nucleotides 16144–16164) tgaccacctgtagtacataa; P6 (nucleotides 16410–16390) gaggatggtggtcaagggac.

The relative proportions of the G6930A mutation in *MTCO1* and the 14787–14790 microdeletion in *MTCytB* were determined in each hybrid clone by PCR–RFLP analysis as described earlier (11,14) using P1–P2 and P3–P4 primers sets, respectively (Fig. 3). Briefly, amplified mtDNA fragments were radiolabeled by the 'last cycle hot' technique (23), digested with *Alu*I (for the G6930A mutation) or *Ase*I (for the 14787–14790 microdeletion), separated on a 12% polyacrylamide gel, and quantified with a Cyclone phosphorimager using the OptiQuant software (Hewlett Packard).

For the sequencing of a fragment of the D-loop region from both parental mtDNA haplotypes, PCR amplification was performed using the P5–P6 primer set. Both strands of the resulting 266 bp fragment were sequenced using an ABI 3700 automated sequencer. Quantification of the relative proportion of the C16278T polymorphism in the D-loop of the hybrids clones was performed on *Eco*RV digestion of PCR products amplified with the P5–P6 primer set and radiolabeled with the 'last cycle hot'. The 7386 bp long mtDNA fragments encompassing both the G6930A and C16278T mutations were amplified with P2–P5 primers using the Expand Long Template System (Roche) according to the manufacturer's protocol, except that the annealing temperature was 61°C. PCR products were subcloned using the TOPO XL PCR Cloning Kit (Invitrogen). Sequencing of the long-PCR subclones was performed using the M13 forward and M13 reverse primers and a series of internal mtDNA primers spanning the entire fragment. PCR–RFLP analyses of the subclones to identify the G6930A and C16278T mutations were performed as described earlier.

Southern blot analysis of mtDNA was performed as described earlier (24). Briefly, ~10 μg of total DNA were digested with the restriction enzymes *Eco*RV and *Ase*I. DNA fragments were separated in a 0.8% agarose gel and transferred to a ZetaProbe membrane (BioRad) according to the manufacturer's protocol. MtDNA was detected with [α–^{32}P]dATP random primed radiolabeled (Random primed DNA labeling kit, Roche) mtDNA fragments (P1 nucleotides 15494–16255 and P2 nucleotides 13714–14749), and hybridizing bands were quantified with a Cyclone phosphorimager, as mentioned earlier.

ACKNOWLEDGEMENTS

We thank Dr Eric Schon, Columbia University, New York, Drs Valeria Tiranti and Massimo Zeviani, Istituto Neurologico Besta, Milan, Italy, for their insightful comments. This work was supported by grants from the United Mitochondrial Disease foundation US National Institutes of Health (NS02179 to G.M., GM55766 and EY10804 to C.T.M.) and the Muscular Dystrophy Association (G.M.).

REFERENCES

1. Gray, M.W. (1989) Origin and evolution of mitochondrial DNA. *Annu. Rev. Cell Biol.*, **5**, 25–50.
2. Ladoukakis, E.D. and Zouros, E. (2001) Direct evidence for homologous recombination in mussel (*Mytilus galloprovincialis*) mitochondrial DNA. *Mol. Biol. Evol.*, **18**, 1168–1175.
3. Thyagarajan, B., Padua, R.A. and Campbell, C. (1996) Mammalian mitochondria possess homologous DNA recombination activity. *J. Biol. Chem.*, **271**, 27536–27543.
4. Tang, Y., Manfredi, G., Hirano, M. and Schon, E.A. (2000) Maintenance of human rearranged mitochondrial DNAs in long-term cultured transmitochondrial cell lines. *Mol. Biol. Cell*, **11**, 2349–2358.
5. Holt, I.J., Dunbar, D.R. and Jacobs, H.T. (1997) Behaviour of a population of partially duplicated mitochondrial DNA molecules in cell culture:

segregation, maintenance and recombination dependent upon nuclear background. *Hum. Mol. Genet.*, **6**, 1251–1260.
6. Eyre-Walker, A. and Awadalla, P. (2001) Does human mtDNA recombine? *J. Mol. Evol.*, **53**, 430–435.
7. Hagelberg, E. (2003) Recombination or mutation rate heterogeneity? Implications for mitochondrial Eve. *Trends Genet.*, **19**, 84–90.
8. Piganeau, G. and Eyre-Walker, A. (2004) A reanalysis of the indirect evidence for recombination in human mitochondrial DNA. *Heredity*, **92**, 282–288.
9. Kraytsberg, Y., Schwartz, M., Brown, T.A., Ebralidse, K., Kunz, W.S., Clayton, D.A., Vissing, J. and Khrapko, K. (2004) Recombination of human mitochondrial DNA. *Science*, **304**, 981.
10. King, M.P. and Attardi, G. (1989) Human cells lacking mtDNA: repopulation with exogenous mitochondria by complementation. *Science*, **246**, 500–503.
11. Bruno, C., Martinuzzi, A., Tang, Y., Andreu, A.L., Pallotti, F., Bonilla, E., Shanske, S., Fu, J., Sue, C.M., Angelini, C. *et al.* (1999) A stop-codon mutation in the human mtDNA cytochrome *c* oxidase I gene disrupts the functional structure of complex IV. *Am. J. Hum. Genet.*, **65**, 611–620.
12. D'Aurelio, M., Pallotti, F., Barrientos, A., Gajewski, C.D., Kwong, J.Q., Bruno, C., Beal, M.F. and Manfredi, G. (2001) *In vivo* regulation of oxidative phosphorylation in cells harboring a stop-codon mutation in mitochondrial DNA-encoded cytochrome *c* oxidase subunit I. *J. Biol. Chem.*, **276**, 46925–46932.
13. De Coo, I.F., Renier, W.O., Ruitenbeek, W., Ter Laak, H.J., Bakker, M., Schagger, H., Van Oost, B.A. and Smeets, H.J. (1999) A 4-base pair deletion in the mitochondrial cytochrome *b* gene associated with parkinsonism/MELAS overlap syndrome. *Ann. Neurol.*, **45**, 130–133.
14. Rana, M., de Coo, I., Diaz, F., Smeets, H. and Moraes, C.T. (2000) An out-of-frame cytochrome *b* gene deletion from a patient with parkinsonism is associated with impaired complex III assembly and an increase in free radical production. *Ann. Neurol.*, **48**, 774–781.
15. Drouin, J. (1980) Cloning of human mitochondrial DNA in *Escherichia coli. J. Mol. Biol.*, **140**, 15–34.
16. Yoon, Y.G. and Koob, M.D. (2003) Efficient cloning and engineering of entire mitochondrial genomes in *Escherichia coli* and transfer into transcriptionally active mitochondria. *Nucl. Acids Res.*, **31**, 1407–1415.
17. King, M.P. (1996) Use of ethidium bromide to manipulate ratio of mutated and wild-type mitochondrial DNA in cultured cells. *Methods Enzymol.*, **264**, 339–344.
18. Kagawa, W., Kurumizaka, H., Ikawa, S., Yokoyama, S. and Shibata, T. (2001) Homologous pairing promoted by the human Rad52 protein. *J. Biol. Chem.*, **276**, 35201–35208.
19. Legros, F., Lombes, A., Frachon, P. and Rojo, M. (2002) Mitochondrial fusion in human cells is efficient, requires the inner membrane potential, and is mediated by mitofusins. *Mol. Biol. Cell*, **13**, 4343–4354.
20. Jacobs, H.T., Lehtinen, S.K. and Spelbrink, J.N. (2000) No sex please, we're mitochondria: a hypothesis on the somatic unit of inheritance of mammalian mtDNA. *Bioessays*, **22**, 564–572.
21. Legros, F., Malka, F., Frachon, P., Lombes, A. and Rojo, M. (2004) Organization and dynamics of human mitochondrial DNA. *J. Cell Sci.*, **117**, 2653–2662.
22. Iborra, F.J., Kimura, H. and Cook, P.R. (2004) The functional organization of mitochondrial genomes in human cells. *BMC Biol.*, **2**, 9.
23. Moraes, C.T., Ricci, E., Bonilla, E., DiMauro, S. and Schon, E.A. (1992) The mitochondrial tRNA(Leu(UUR)) mutation in mitochondrial encephalomyopathy, lactic acidosis, and strokelike episodes (MELAS): genetic, biochemical, and morphological correlations in skeletal muscle. *Am. J. Hum. Genet.*, **50**, 934–949.
24. Zeviani, M., Moraes, C.T., DiMauro, S., Nakase, H., Bonilla, E., Schon, E.A. and Rowland, L.P. (1988) Deletions of mitochondrial DNA in Kearns–Sayre syndrome. *Neurology*, **38**, 1339–1346.